Bipolar coordinates, image method and the method of fundamental solutions for Green's functions of Laplace problems containing circular boundaries

J.T. Chen [a,b,*], H.C. Shieh [a], Y.T. Lee [a], J.W. Lee [a]

[a] Department of Harbor and River Engineering, National Taiwan Ocean University, Keelung 20224, Taiwan
[b] Department of Mechanical and Mechatronic Engineering, National Taiwan Ocean University, Keelung 20224, Taiwan

ARTICLE INFO

ABSTRACT

Green's functions of Laplace problems containing circular boundaries are solved by using analytical and semi-analytical approaches. For the analytical solution, we derive the Green's function using the bipolar coordinates. Based on the semi-analytical approach of image method, it is interesting to find that the two frozen images for the eccentric annulus using the image method are located on the two foci in the bipolar coordinates. This finding also occurs for the cases of a half plane with a circular hole and an infinite plane containing two circular holes. The image method can be seen as a special case of the method of fundamental solutions, which only at most four unknown strengths are required to be determined. The optimal locations of sources in the method of fundamental solutions can be captured using the image method and they are dependent on the source location and the geometry of problems. Three illustrative examples were demonstrated to verify this point. Results are satisfactory.

1. Introduction

A number of physical and engineering problems governed by the Lapalce equation in two independent variables, e.g., steady-state heat conduction, electrostatic potential and fluid flow, were solved using the conformal mapping to obtain an analytical solution. Besides, we can formulate the same problems using special curvilinear coordinates to obtain a solution, e.g., bipolar coordinates and elliptic coordinates. Carrier and Pearson [1] employed the bilinear transformation of conformal mapping to solve certain kinds of potential problems. An eccentric case was mapped to an annular domain through a bilinear transformation. For a polygonal shape, it can also be mapped to a regular region using the Schwarz–Christoffel transformation [2]. For a regular geometry, it is easy to solve the Laplace problem using the polar or Cartesian coordinates. Muskhelishvili [3] gave us a detailed description how an eccentric annulus can be mapped into a concentric annulus using a simple form of linear fractional transformation. Chen and Weng [4] also used a similar method to solve eccentric annulus problems. Although a bilinear transformation was used, the mapping functions were not exactly the same between the one of Carrier and Pearson [1] and that of Muskhelishvili [3]. Problems of eccentric annulus, a half plane with a circular hole or an infinite plane containing two circular holes were usually solved by using the bipolar coordinates

to derive the analytical solution [5]. Ling [6], Timoshenko and Goodier [7], and Lebedev et al. [8] all presented an analytic solution by using the bipolar coordinates for the torsion problem of an eccentric bar. However, the mapping functions were not exactly the same. One is a cotangent function [6], another is a hyperbolic tangent function [8] and the other is a hyperbolic cotangent function [7]. After the bipolar coordinate system is introduced, the problem of special domain can be solved by using the separation of variables. Although Carrier and Pearson [1], Muskhelishvili [3], Ling [6], Timoshenko and Goordier [7] have solved the eccentric Laplace problems, their approaches are very similar, but not identical. Chen et al. [9] found that all the above-mentioned approaches can be unified after suitable transformations, translation, rotation and taking log in the conformal mapping. However, we will focus on Green's function instead of BVP without sources [10] in this paper.

Green's function has been studied and applied in science and engineering by mathematicians as well as engineers, respectively [11]. A computer-friendly solution for the potential generated by a point source in the ring-shaped region was studied by Melnikov and Arman [12]. In order to derive Green's function, Thomson [13] proposed the concept of reciprocal radii to find the image source to satisfy the homogeneous Dirichlet boundary condition using the image method. Greenberg [14] and Riley et al. [15] employed a trick to satisfy the boundary condition for two special points, then the image location can be determined. Chen and Wu [16] proposed a natural and logical way to find the location of image and the strength by employing the degenerate kernel. The image method is a classical approach for constructing Green's function. In certain cases, it is possible to obtain the exact solution for a concentrated source in a bounded domain through

* Corresponding author at: Department of Harbor and River Engineering, National Taiwan Ocean University, Keelung 20224, Taiwan.
Tel.: +886 2 24622192x6177; fax: +886 2 24632375.
E-mail address: jtchen@mail.ntou.edu.tw (J.T. Chen).

superimposing the infinite plane solution for the given source and its image source. Although the scope of this method is limited, it yields a great deal of insight into the solution when it works [17]. Here, we will extend to a semi-analytical approach once the closed-form solution using the image method is not possible. Our goal is to broaden the scope of applications on the image method.

In this paper, we have three issues. First, the image method is seen as a special case of the method of fundamental solutions since its image singularities locate outside the domain. Second, the optimal locations of the method of fundamental solutions sources are found to be dependent on the source location and the geometry of the problems. Third, it is found that the two frozen images of the image method are located on the two foci in the bipolar coordinates. Using the bipolar coordinates and the image method, three cases, an eccentric annulus, a half plane with a circular hole and an infinite domain containing two circular holes, are solved. The bipolar coordinates are reviewed for the eccentric ring in Section 2. In Section 3, the image method is employed to derive Green's function for problems containing circular boundaries. Numerical results are given in Section 4. Finally, a conclusion is drawn in Section 5.

2. Geometric characterization of the bipolar coordinates

The relation between the bipolar coordinates (ξ, η) and the Cartesian coordinates (x, y) [9] is defined by

$$x + iy = ic\cot\left(\frac{1}{2}\zeta\right), \quad \zeta = \xi + i\eta, \tag{1}$$

where c is a positive constant. Eq. (1) yields

$$x = c\frac{\sinh\eta}{\cosh\eta - \cos\xi}, \quad y = c\frac{\sin\xi}{\cosh\eta - \cos\xi}, \tag{2}$$

where $-\pi \le \xi < \pi, -\infty < \eta < \infty$. By eliminating ξ in Eq. (2), we obtain a circle with the center at $(c\coth\eta, 0)$ and the radius $c\,\mathrm{csch}\eta$ as follows:

$$(x - c\coth\eta)^2 + y^2 = c^2\mathrm{csch}^2\eta. \tag{3}$$

Elimination of η from Eq. (2) results in the other circle with the center at $(0, c\cot\xi)$ and the radius of $c\csc\xi$ as follows:

$$x^2 + (y - c\cot(\xi))^2 = c^2\csc^2(\xi). \tag{4}$$

Denoting by (Γ_1, φ_1) and (Γ_2, φ_2), we have

$$x + iy + c = \Gamma_1 e^{i\varphi_1}, \quad x + iy - c = \Gamma_2 e^{i\varphi_2}, \tag{5}$$

$$\eta = \log(\Gamma_1/\Gamma_2), \quad \xi = \varphi_2 - \varphi_1. \tag{6}$$

It follows that a curve $\xi = $ constant is a family of circles passing through the poles $(\pm c, 0)$. The curve of $\eta = $ constant shows a curve for which $\Gamma_1/\Gamma_2 = $ constant. The eccentric annulus is shown in Fig. 1. The outer radius b, inner radius a and the distance d are determined from Eq. (3) as follows:

$$a = c\,\mathrm{csch}(\eta_1), \tag{7}$$

$$b = c\,\mathrm{csch}(\eta_2), \tag{8}$$
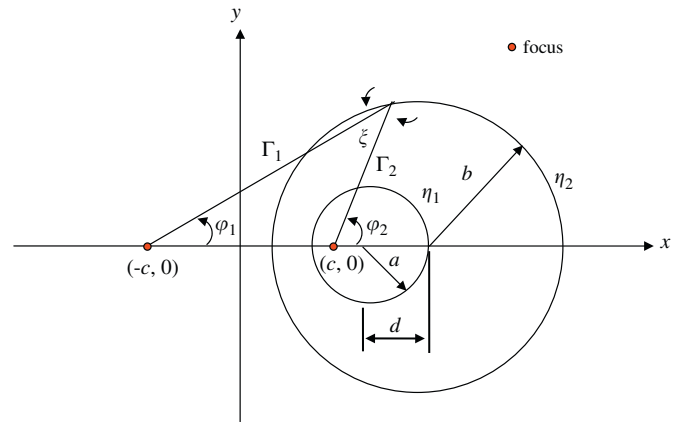
$$d = c[\coth(\eta_2) - \coth(\eta_1)]. \tag{9}$$

Fig. 1. Geometry relation of bipolar coordinates.

To describe an eccentric annulus in the bipolar coordinates, the three parameters, c, η_1 and η_2 are determined as follows:

$$c = \frac{\sqrt{a^4 + b^4 - 2a^2b^2 - 2d^2(a^2 + b^2) + d^4}}{2d}, \tag{10}$$

$$\eta_1 = \sinh^{-1}\left(\frac{c}{a}\right), \tag{11}$$

$$\eta_2 = \sinh^{-1}\left(\frac{c}{b}\right), \tag{12}$$

where η_1 and η_2 denote the inner and outer circles, respectively. Then, we can describe an eccentric annulus using the bipolar coordinates. In this case, Green's function was derived in terms of the bipolar coordinates as shown below [5]

$$G(\xi, \eta; \xi_0, \eta_0) = \begin{cases} \frac{1}{2\pi}\left[\frac{(\eta_1 - \eta)(\eta_2 - \eta_0)}{\eta_1 - \eta_2} + 2\sum_{n=1}^{\infty}\frac{\sinh n(\eta_1 - \eta)\sinh n(\eta_2 - \eta_0)}{n\sinh n(\eta_1 - \eta_2)}\cos n(\xi - \xi_0)\right], & \eta_1 \ge \eta \ge \eta_0, \\ \frac{1}{2\pi}\left[\frac{(\eta - \eta_2)(\eta_0 - \eta_1)}{\eta_1 - \eta_2} + 2\sum_{n=1}^{\infty}\frac{\sinh n(\eta_2 - \eta)\sinh n(\eta_1 - \eta_0)}{n\sinh n(\eta_1 - \eta_2)}\cos n(\xi - \xi_0)\right], & \eta_0 \ge \eta \ge \eta_2, \end{cases} \tag{13}$$

where (ξ_0, η_0) is the position of the source point.

3. Image method

For a problem of two-dimensional eccentric annulus as shown in Fig. 2, Green's function $G(x, s)$ satisfies

$$\nabla^2 G(x, s) = \delta(x - s), \quad x \in \Omega, \tag{14}$$

where Ω is the domain of interest, x is the field point and δ denotes the Dirac-delta function for the source at s. For simplicity, Green's function is considered to be subject to the homogeneous Dirichlet boundary conditions. In this case, we obtain the location of image point using the fundamental solution and matching the boundary condition. The eccentric annulus can be seen as a combination of interior and exterior problems as shown in Fig. 3. The source point and the image point are s and s' in Fig. 3, respectively. By matching the homogeneous Dirichlet boundary conditions for the interior or exterior boundaries, the position of the image source is at $(a^2/R_s, \theta)$, where $s = (R_s, \theta)$. We consider the fundamental solution $U(x, s)$ for the infinite plane that is governed

by

$$\nabla^2 U(x,s) = 2\pi\delta(x-s). \tag{15}$$

The closed-form fundamental solution is given as

$$U(x,s) = \ln r, \tag{16}$$

where r is the distance between s and x ($r \equiv |x-s|$). Based on the separable property of the addition theorem or the so-called degenerate kernel, the fundamental solution $U(x,s)$ can be expanded into a series form by separating the field point $x(\rho, \phi)$ and the source point $s(R_s, \theta)$ in the polar coordinates

$$U(x,s) = \begin{cases} U^I(\rho,\phi;R_s,\theta) = \ln R_s - \sum_{m=1}^{\infty} \dfrac{1}{m}\left(\dfrac{\rho}{R_s}\right)^m \cos m(\theta-\phi), & R_s \geq \rho, \\ U^E(\rho,\phi;R_s,\theta) = \ln\rho - \sum_{m=1}^{\infty} \dfrac{1}{m}\left(\dfrac{R_s}{\rho}\right)^m \cos m(\theta-\phi), & R_s < \rho. \end{cases} \tag{17}$$

The image method can solve Green's function of eccentric case in a semi-analytical manner. Following the successive image process, it is found that the final two image locations freeze at the s_{c1} and s_{c2}. For the eccentric case, the distance from the center of

Fig. 2. Problem sketch for Green's function of an eccentric annulus.

outer circle to the source is $R_s = \sqrt{x_0^2 + y_0^2}$. The successive former four locations of images are

$$R_1 = \frac{b^2}{R_s}, \quad x_1 = R_1\cos\theta_1, \quad y_1 = R_1\sin\theta_1,$$

$$R_2 = \frac{a^2}{\sqrt{(x_0+d)^2 + y_0^2}}, \quad x_2 = R_2\cos\theta_2 - d, \quad y_2 = R_2\sin\theta_2,$$

$$R_3 = \frac{b^2}{\sqrt{x_2^2 + y_2^2}}, \quad x_3 = R_3\cos\theta_3, \quad y_3 = R_3\sin\theta_3,$$

$$R_4 = \frac{a^2}{\sqrt{(x_1+d)^2 + y_1^2}}, \quad x_4 = R_4\cos\theta_4 - d, \quad y_4 = R_4\sin\theta_4, \tag{18}$$

$$\theta_1 = \theta,$$
$$\theta_2 = \tan^{-1}\left(\frac{y_2}{x_2+d}\right),$$
$$\theta_3 = \tan^{-1}\left(\frac{y_3}{x_3}\right),$$
$$\theta_4 = \tan^{-1}\left(\frac{y_4}{x_4+d}\right), \tag{19}$$

Green's functions for the two cases: (a) an eccentric annulus and (b) a half plane containing a circular hole, can be represented by

$$G(x,s) = \frac{1}{2\pi}\left\{\ln|x-s| - \lim_{N\to\infty}\left[\sum_{i=1}^{N}(\ln|x-s_{4i-3}| + \ln|x-s_{4i-2}| - \ln|x \right.\right.$$
$$\left.\left. -s_{4i-1}| - \ln|x-s_{4i}|) + c_1(N)\ln|x-s_{c_1}| + c_2(N)\ln|x-s_{c_2}| + e(N)\right]\right\}, \tag{20}$$

where s_{4i-3}, s_{4i-2}, s_{4i-1} and s_{4i} are the successive image locations [18], $e(N)$ can be understood as a rigid body term, $c_1(N)$ and $c_2(N)$ are the singularity strengths of the two frozen points at s_{c1} and s_{c2}, which can be determined by matching the boundary conditions. For the case of infinite plane containing two circular holes, the expression of Green's function is given in Table 1. Table 1 demonstrates that the frozen image points s_{c1} and s_{c2} happen to be two foci in the bipolar coordinates.
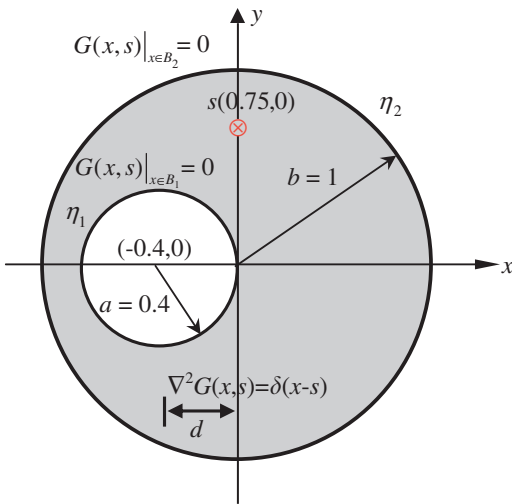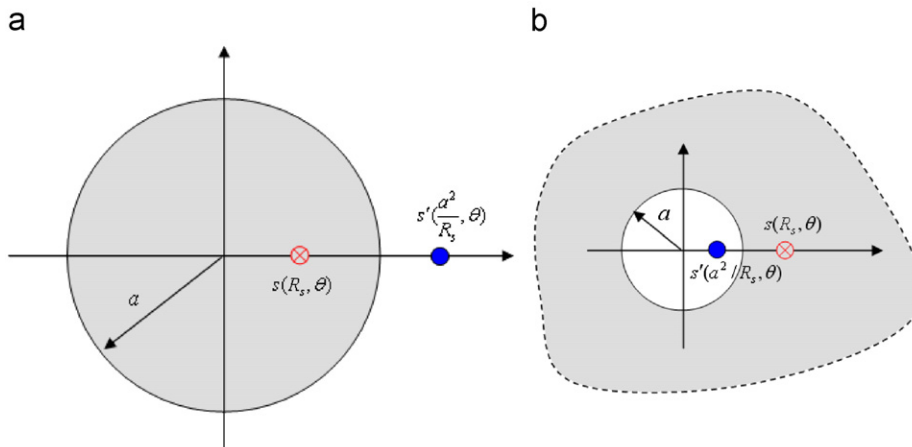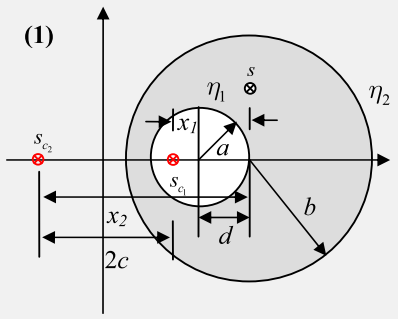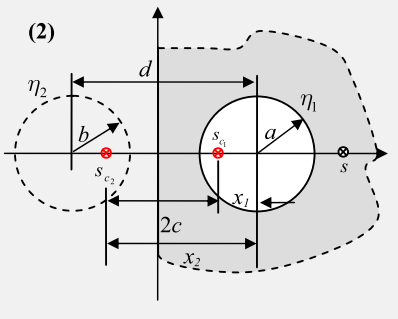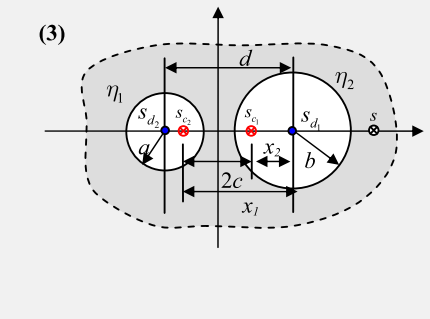

Fig. 3. Sketch of position of image point (a) an interior case and (b) an exterior case.

Table 1
Frozen points of the image method and foci in the bipolar coordinates.

Method	Cases		
	(1)	**(2)**	**(3)**

Image method

Case (1):

$$G(x,s) = \frac{1}{2\pi}\left\{ \ln|x-s| + \lim_{N\to\infty}\left[\left(\sum_{m=1}^{N} -\ln|x-s_{4i-3}| - \ln|x-s_{4i-2}| + \ln|x-s_{4i-1}|\right.\right.\right.$$
$$\left.\left.\left. + \ln|x-s_{4i}|\right) + c_1(N)\ln|x-s_{c_1}| + c_2(N)\ln|x-s_{c_2}| + e(N)\right]\right\}$$

Case (3):

$$G(x,s) = \frac{1}{2\pi}\left\{ \ln|x-s| + \lim_{N\to\infty}\left[\left(\sum_{i=1}^{N} \ln|x-s_{2i-1}|\right.\right.\right.$$
$$\left.\left.\left. + \ln|x-s_{2i}|\right) + c_1(N)\ln|x-s_{c_1}| + c_2(N)\ln|x-s_{c_2}|\right]\right.$$
$$\left. + d_1\left[\ln|x-s_{d1}| + \lim_{M\to\infty}\sum_{j=1}^{M}\ln|x-s_j^1|\right]\right.$$
$$\left. + d_2\left[\ln|x-s_{d2}| + \lim_{M\to\infty}\sum_{j=1}^{M}\ln|x-s_j^2|\right]\right\}$$

Bipolar coordinates

Case (1):
$$x_1 - d = \frac{a^2}{x_2 - d}, \quad x_2 = \frac{b^2}{x_1 + d}$$

Case (2):
$$x_1 = \frac{a^2}{x_2}, \quad x_2 = d - x_1, \text{ when } b = a$$
$$c = \frac{(x_2 - x_1)}{2} = \frac{\sqrt{a^4 - 2a^2 b^2 + b^4 - 2a^2 d^2 - 2b^2 d^2 + d^4}}{2d} \Rightarrow \frac{\sqrt{d^2 - 4a^2}}{2}(a = b)$$

Case (3):
$$d - x_1 = \frac{a^2}{d - x_2}, \quad x_2 = \frac{b^2}{x_1}$$
$$c = \frac{\sqrt{a^4 - 2a^2 b^2 + b^4 - 2a^2 d^2 - 2b^2 d^2 + d^4}}{2d}$$
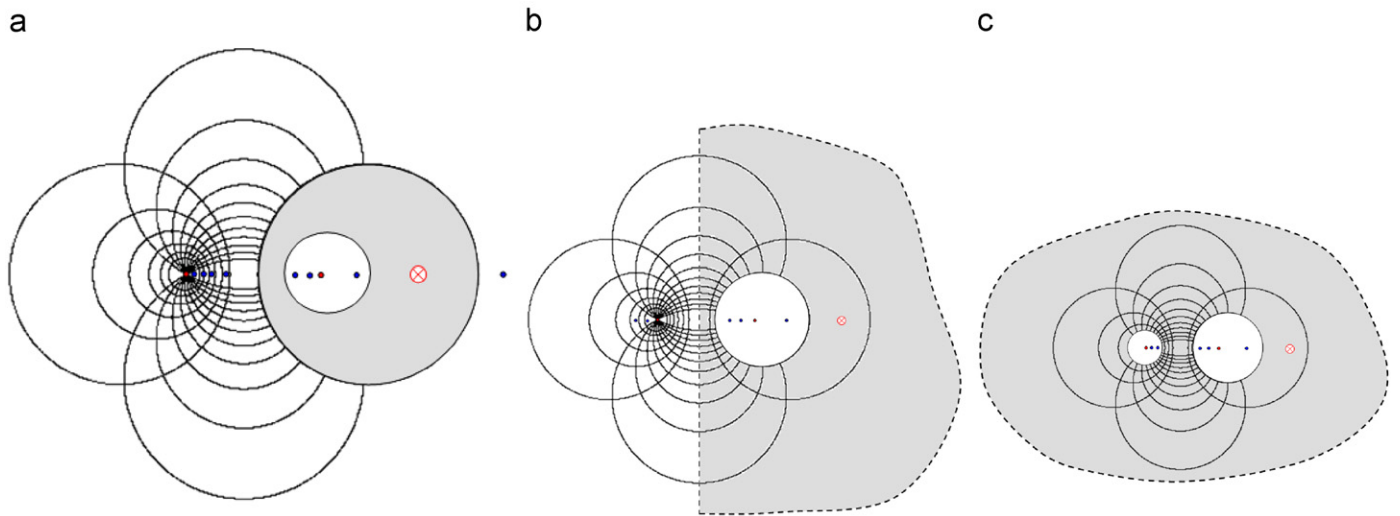

Fig. 4. Final images and the foci of the bipolar coordinates (a) an eccentric annulus, (b) a half plane containing a circular hole and (c) an infinite plane with two circular holes.

4. Illustrative examples

Case 1. An eccentric case (a special case: annular case [12])

The problem sketch of an eccentric annulus is shown in Fig. 2. The location of image source and bipolar coordinates are shown in Fig. 4(a). The source point is located at $s = (0, 0.75)$. The centers of two holes are set at $(0, 0)$ and $(-0.4, 0)$, and the radii are 0.4 and 1.0 for the inner and outer boundaries, respectively. Following the success of annulus case for the iterative images, we now extend to the eccentric case. In a similar way of finding the successive images for matching the inner and outer boundary conditions [18], the solution can be superimposed using Eq.(20). Finally, we

can find that the final frozen image points and the foci of the bipolar coordinates are the same. After collocating some points to match the boundary conditions, all the unknown coefficients can be determined. The results are compared well with the analytical solution using the bipolar coordinates. The contour plots using the present method of Eq. (20), the bipolar coordinates of Eq. (13) and the null-field BIEM [19] are shown in Fig. 5.

Case 2. A half plane containing a circular hole

Fig. 4(b) depicts Green's function for the half plane containing a circular hole and the homogeneous Dirichlet boundary condition. The source point is located at $s = (3, 0)$. The center and radius of the
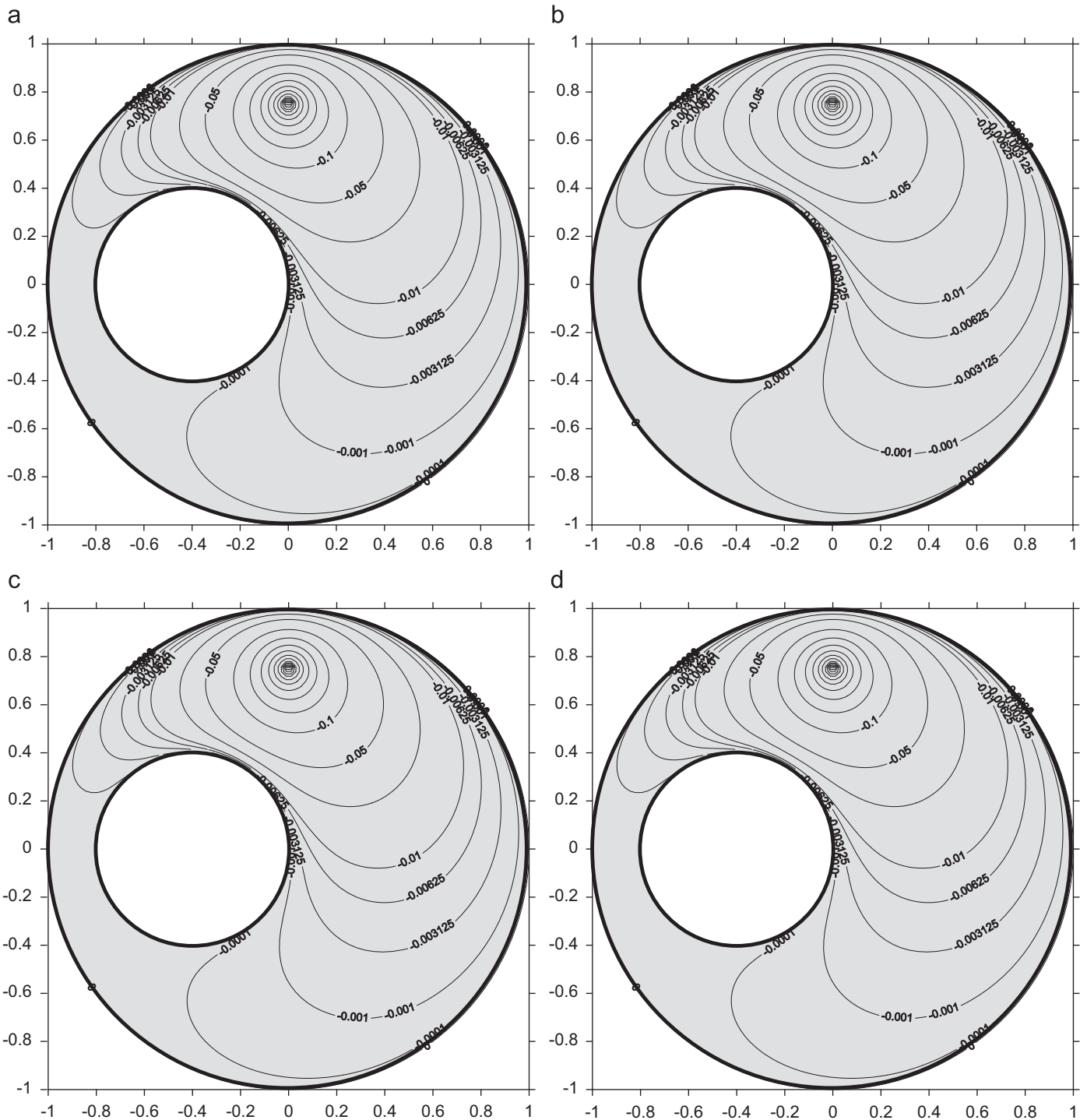
Fig. 5. Green's function using (a) an analytical solution using the bipolar coordinates, (b) an image solution, (c) a solution using the superposition technique and the null-field BIEM [18,19] and (d) solution using Green's third identity in the null-field BIEM.

circular hole is (1.25,0) and $a=1$, respectively. The $d/2=1.25$ is the distance from the center to the ground line. Similarly, the analytical and semi-analytical solutions are obtained using the bipolar coordinates and the image method, respectively. The results agree well with those of the null-field BIEM [18,19] in Fig. 6.

Case 3. An infinite plane containing two circular holes

Following the successful experiences of the eccentric annulus case for the iterative images, we now extend to the infinite plane containing two circular holes as shown in Table 1. The

problem sketch of the infinite plane containing two circular holes is shown in Fig. 4(c). The source point is located at $s=(3.85,0)$. The centers of two holes are set at $(0,0)$ and $(2.1,0)$, and their radii are 0.4 and 1, respectively. In a similar way of finding the image sources for matching boundary conditions [18], an image solution is derived.

We also found that the final frozen image points approach to the foci of the bipolar coordinates. Based on the image solution for an infinite plane containing a circular hole subject to the homogeneous Neumann BC, an extra source at the center of hole
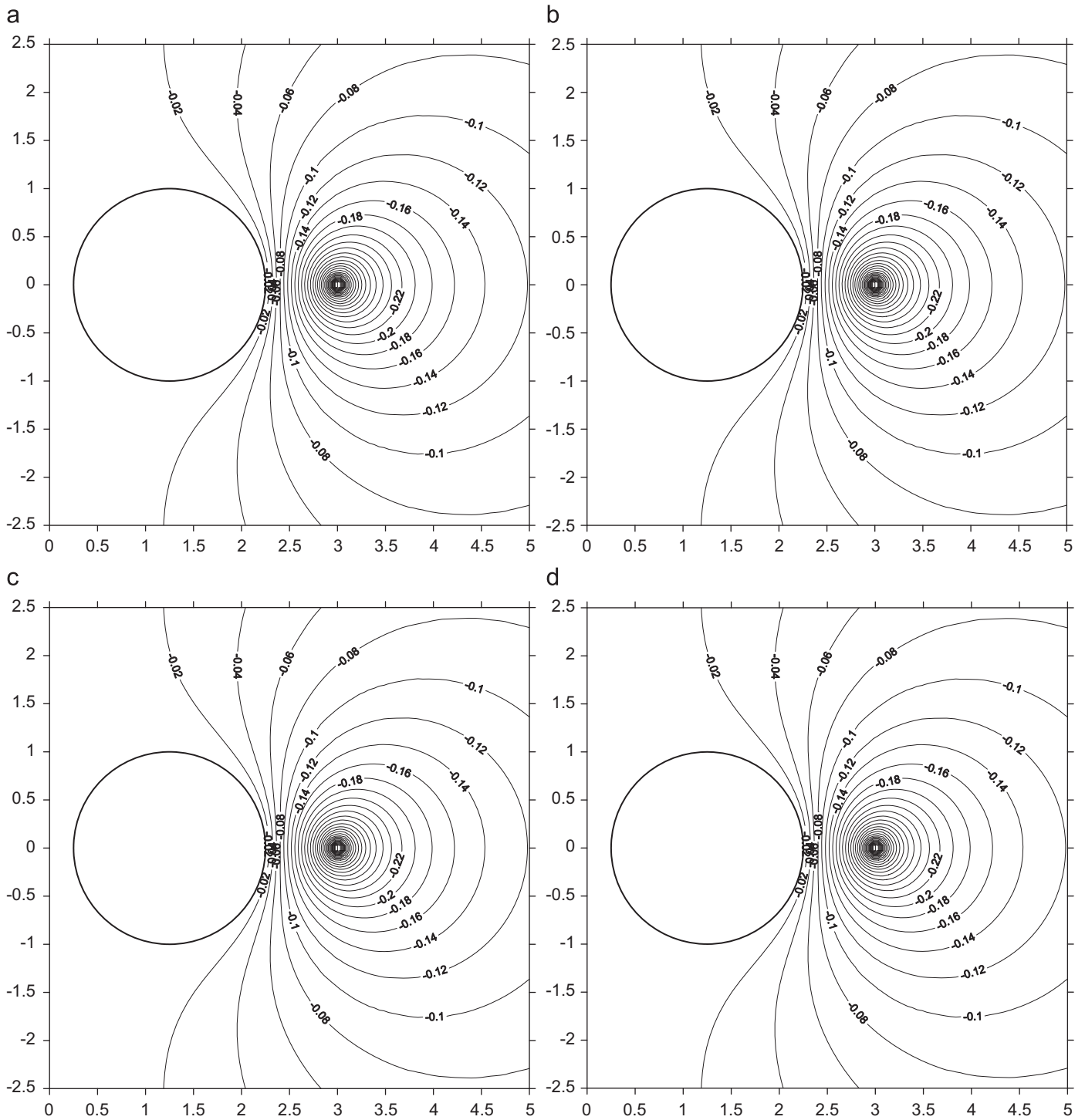
a

b

c

d

Fig. 6. Green's function using (a) an analytical solution using the bipolar coordinates, (b) an image solution, (c) a solution using the superposition technique and the null-field BIEM [18,19] and (d) solution using Green's third identity in the null-field BIEM.

is required. This motivates us to put sources at two centers of the holes to obtain acceptable results. Therefore, Eq. (20) is extended to

$$G(x,s) = \frac{1}{2\pi}\left\{ \ln|x-s| + \lim_{N \to \infty}\left[\left(\sum_{i=1}^{N} \ln|x-s_{2i-1}| + \ln|x-s_{2i}| \right) \right.\right.$$

$$\left. + c_1(N)\ln|x-s_{c_1}| + c_2(N)\ln|x-s_{c_2}| \right]$$

$$+ d_1\left[\ln|x-s_{d1}| + \lim_{M \to \infty}\sum_{j=1}^{M} \ln|x-s_j^1| \right]$$

$$\left. + d_2\left[\ln|x-s_{d2}| + \lim_{M \to \infty}\sum_{j=1}^{M} \ln|x-s_j^2| \right] \right\}, \qquad (21)$$

where two extra sources s_{d1} and s_{d2} are located at the two centers of holes, s_j^1 and s_j^2 are the successive images due to s_{d1} and s_{d2}, respectively. The results agree well with those of the
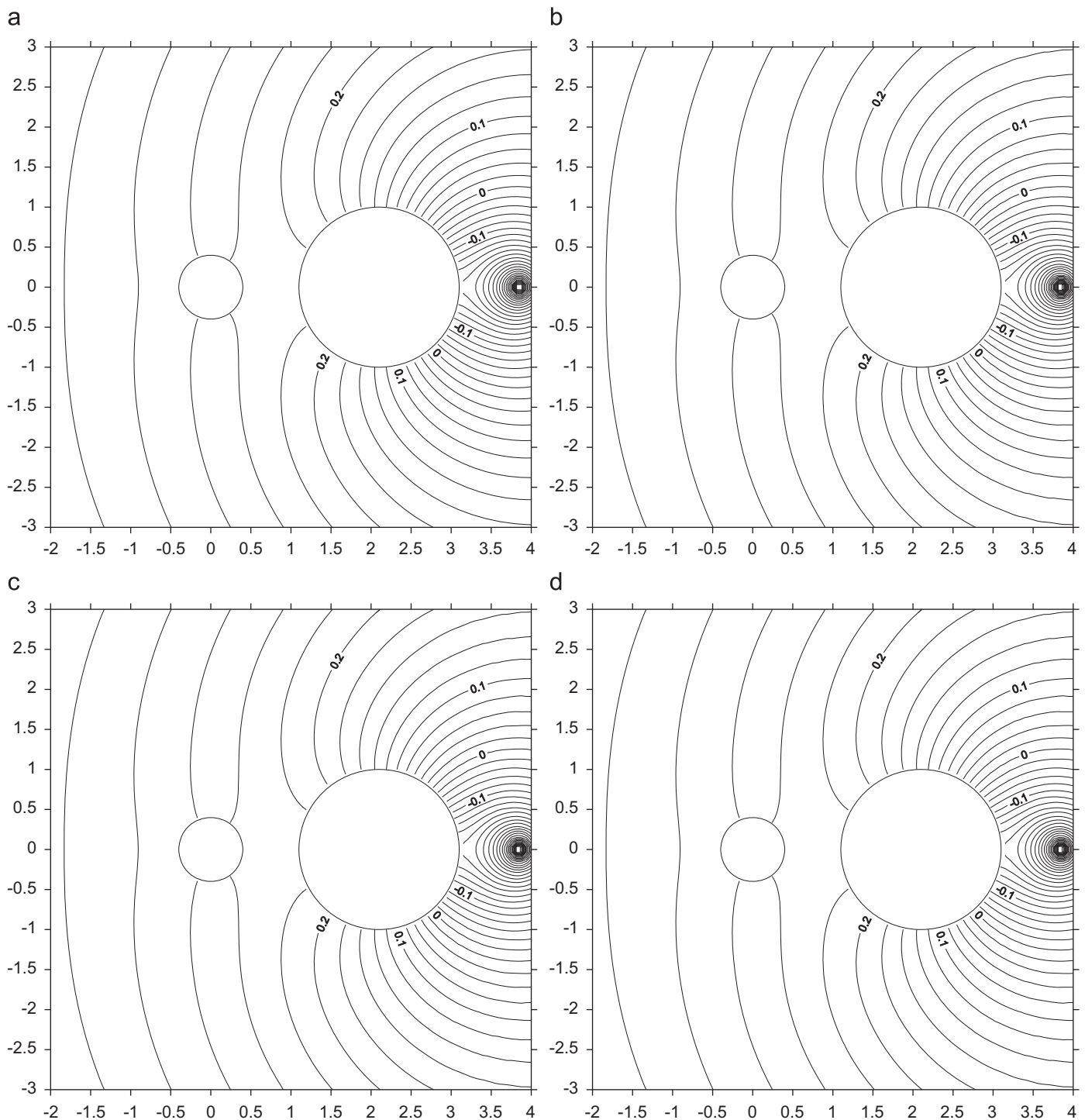
a

b

c

d

Fig. 7. Green's function using (a) an analytical solution using the bipolar coordinates, (b) an image solution, (c) a solution using the superposition technique and the null-field BIEM [18,19] and (d) solution using Green's third identity in the null-field BIEM.

null-field BIEM [18,19] and the conventional MFS in Fig. 7. It is interesting to find that the final images also freeze at foci in the bipolar coordinates. The results are summarized in Table 1.

For arbitrary boundaries, it is not easy to have such a neat semi-analytical solution. Furthermore, the simple case is extension to a straight boundary and can be found in textbooks. Our approach can also be easily extended to solve inclusion problems by taking free body. One part is a boundary value problem without a source, the other is also a BVP with a source. Additionally, matching the boundary conditions on the interface is required.

5. Conclusions

In this paper, Green's functions were derived using the image method. It is found that final image points terminate at the two foci of the bipolar coordinates for all the three cases, an eccentric annulus, a half plane containing a circular hole and an infinite plane containing two circular holes. The optimal source distribution in the MFS is dependent on the given geometry and the source location. An image method can guide us to search for an optimal source location of the MFS and can determine the

strengths of sources except the two frozen images. Three examples were demonstrated to find all the image sources for constructing Green's function. The dimension of the influence matrix in the linear algebraic equation is at most four by four in all the examples. Agreement is made after comparing with other solutions.

Acknowledgements

References

[1] Carrier GF, Pearson CE. Partial differential equation—theory and technique. New York: Academic Press; 1976.

[2] Lafe OE, Montes JS, Cheng AHD, Liggett JA, Liu PL-F. Singularity in Darcy flow through porous media. J Hydraul Div 1980;106:977–97.

[3] Muskhelishvili NI. Some basic problems of the mathematical theory of elasticity. Groningen: Noordhoff; 1953.

[4] Chen T, Weng IS. Torsion of a circular compound bar with imperfect interface. J Appl MechTrans ASME 2001;68:955–8.

[5] Heyda JF. A Green's function solution for the case of laminar incompressible flow between non-concentric cylinders. J Franklin Inst 1959;267:25–34.

[6] Ling CB. Torsion of an eccentric circular tube. Technical Report. No.1, Chinese Bureau of Aeronautical Research., 1940.

[7] Timoshenko SP, Goodier JN. Theory of elasticity. New York: McGraw-Hill; 1972.

[8] Lebedev NN, Skalskaya IP, Uflyand YS. Worked problems in applied mathematics. New York: Dover; 1965.

[9] Chen JT, Tsai MH, Liu CS. Conformal mapping and bipolar coordinate for eccentric Laplace problems. Comput Appl Eng Educ 2009;17:314–22.

[10] Chen JT, Shieh HC, Lee YT, Lee JW. Image solutions for boundary value problems without sources. Appl Math Comput 2010;216:1453–68.

[11] Melnikov YA. Some applications of the Green's function method in mechanics. Int J Solids Struct 1977;3:1045–58.

[12] Melnikov YA, Arman A. The fields of potential generated by a point source in the ring-shaped region. Math Eng Ind 2001;3:223–38.

[13] Thomson W. Maxwell in his treatise, quotes a paper in the Cambridge and Dublin Mathematical Journal of 1848, vol. I. Chapter XI., 1848.

[14] Greenberg MD. Application of Green's function in science and engineering. New Jersey: Prentice-Hill; 1971.

[15] Riley KF, Hobson MP, Bence SJ. Mathematical methods for physics and engineering. New York: Cambridge; 2006.

[16] Chen JT, Wu CS. Alternative derivations for the Poisson integral formula. Int J Math Educ Sci Technol 2006;37:165–85.

[17] Keller JB. Progress and prospects in the theory of linear wave propagation. SIAM J Numer Anal 1979;21(2):229–45.

[18] Chen JT, Lee YT, Yu SR, Shieh SC. Equivalence between Trefftz method and method of fundamental solution for the annular Green's function using the addition theorem and image concept. Eng Anal Bound Elem 2009;33: 678–88.

[19] Chen JT, Chou KH, Kao SK. Derivation of Green's function using addition theorem. Mech Res Commun 2009;36:351–63.